Influence of the Peripheral Ligand Atoms on the Exchange Interaction in Oxalato-Bridged Nickel(II) Complexes: An Orbital Model. Crystal Structures and Magnetic Properties of $(H_3dien)_2[Ni_2(ox)_5]\cdot 12H_2O$ and $[Ni_2(dien)_2(H_2O)_2(ox)]Cl_2$

Pascual Román,*[1a] Carmen Guzmán-Miralles,[1a] Antonio Luque,[1a] Javier I. Beitia,[1a] Juan Cano,[1b] Francesc Lloret,*[1b] Miguel Julve,[1b] and Santiago Alvarez[1c]

Departamento de Química Inorgánica, Universidad del País Vasco, Apartado 644, 48080 Bilbao, Spain, Departament de Química Inorgànica, Facultat de Química de la Universitat de València, Dr. Moliner 50, 46100 Burjassot, València, Spain, and Departament de Química Inorgànica, Universitat de Barcelona, Diagonal 647, 08028 Barcelona, Spain

Received August 18, 1995[⊗]

Two nickel(II) complexes of formula $(H_3dien)_2[Ni_2(ox)_5]\cdot 12H_2O$ (**1**) and $[Ni_2(dien)_2(H_2O)_2(ox)]Cl_2$ (**2**) (dien = diethylenetriamine and ox = oxalate dianion) have been synthesized and characterized by single-crystal X-ray diffraction. **1** crystallizes in the orthorhombic system, space group *Abnn*, with $a = 15.386(4)$ Å, $b = 15.710(4)$ Å, $c = 17.071(4)$ Å, and $Z = 4$. **2** crystallizes in the monoclinic system, space group $P2_1/c$, with $a = 10.579(1)$ Å, $b = 7.258(1)$ Å, $c = 13.326(1)$ Å, $\beta = 93.52(3)°$, and $Z = 2$. The structures of **1** and **2** consist of dinuclear oxalato-bridged nickel(II) units which contain bidentate oxalate (**1**) and tridentate dien in the *fac*-conformation (**2**) as terminal ligands. Both features, oxalato as a peripheral ligand and dien in the *fac*-conformation (instead of its usual *mer*-conformation), are unprecedented in the coordination chemistry of nickel(II). The nickel atom is six-coordinated in both compounds, the chromophores being NiO_6 (**1**) and NiN_3O_3 (**2**). The Ni−O(ox) bond distances at the bridge (2.072(4) Å in **1** and 2.11(1) and 2.125(9) Å in **2**) are somewhat longer than those concerning the terminal oxalate (2.037(5) and 2.035(3) Å in **1**). Magnetic susceptibility data of **1** and **2** in the temperature range 4.2−300 K show the occurrence of intramolecular antiferromagnetic coupling with $J = -22.8$ (**1**) and -28.8 (**2**) cm^{-1} (J being the parameter of the exchange Hamiltonian $H = -J\mathbf{S}_A\cdot\mathbf{S}_B$). The observed value of $-J$ in the investigated oxalato-bridged nickel(II) complexes, which can vary from 22 to 39 cm^{-1}, is strongly dependent on the nature of the donor atoms from the peripheral ligands. This influence has been analyzed and rationalized through extended Hückel calculations.

Introduction

A significant magnetostructural research work has been devoted to analyze the remarkable ability of the oxalate (ox) bridge to mediate exchange coupling between first-row transition metal ions separated by more than 5.5 Å in both homo-[2−9] and heteropolynuclear[10] compounds during the last 15 years. The analysis of the factors that influence the magnitude of the coupling through oxalato allowed to tune the value of the singlet−triplet energy gap (J) in oxalato-bridged dinuclear copper(II) complexes between 0 and -386 cm^{-1} by playing on the nature of the terminal ligand (tridentate and/or bidentate nitrogen donors),[5a,c,d] taking advantage of the plasticity of the coordination sphere of copper(II). The rich stereochemistry of copper(II) and the fact that it has only one unpaired electron

⊗ Abstract published in *Advance ACS Abstracts,* May 1, 1996.

(1) (a) Universidad del País Vasco. (b) Universitat de València. (c) Universitat de Barcelona.
(2) Kahn, O. In *Molecular Magnetism*; VCH: New York, 1993.
(3) Alvarez, S.; Julve, M.; Verdaguer, M. *Inorg. Chem.* **1990**, *29*, 4500.
(4) Kahn, O. *Angew. Chem., Int. Ed. Engl.* **1985**, *24*, 834.
(5) (a) Felthouse, T. R.; Laskowski, E. J.; Hendrickson, D. N. *Inorg. Chem.* **1977**, *16*, 1077. (b) Girerd, J. J.; Kahn, O.; Verdaguer, M. *Inorg. Chem.* **1980**, *19*, 274. (c) Julve, M.; Verdaguer, M.; Kahn, O.; Gleizes, A.; Philoche-Levisalles, O. *Inorg. Chem.* **1983**, *22*, 368; **1984**, *23*, 3808. (d) Julve, M.; Faus, J.; Verdaguer, M.; Gleizes, A. *J. Am. Chem. Soc.* **1984**, *106*, 8306. (e) Soto, L.; García, J.; Legros, J. P.; Tuchagues, J. P.; Dahan, F.; Fuertes, A. *Inorg. Chem.* **1989**, *28*, 3378. (f) Gleizes, A.; Julve, M.; Verdaguer, M.; Real, J. A.; Faus, J.; Solans, X. *J. Chem. Soc., Dalton Trans.* **1992**, 3209. (g) Oshio, H.; Nagashima, U. *Inorg. Chem.* **1992**, *31*, 3295. (h) De Munno, G.; Julve, M.; Nicoló, F.; Lloret, F.; Faus, J.; Ruiz, R.; Sinn, E. *Angew. Chem., Int. Ed. Engl.* **1993**, *32*, 613.
(6) (a) Duggan, D. M.; Barefield, E. K.; Hendrickson, D. N. *Inorg. Chem.* **1973**, *12*, 985. (b) Zelentsov, V. V.; Chanturiya, L. M.; Pitskhalava, N. I. *Koord. Khim.* **1978**, *4*, 764. (c) Ribas, J.; Monfort, M.; Díaz, C.; Solans, X. *An. Quím.* **1988**, *84*, 186. (d) Battaglia, L. P.; Bianchi, A.; Bonamartini Corradi A.; García-España, E.; Micheloni, M.; Julve, M. *Inorg. Chem.* **1988**, *27*, 4174. (e) Bencini, A.; Bianchi, A.; García-España, E.; Jeannin, Y.; Julve, M.; Marcelino, V; Philoche-Levisalles, M. *Inorg. Chem.* **1990**, *29*, 963. (f) Bencini, A.; Bianchi, A.; Paoli, P.; García-España, E.; Julve, M.; Marcelino, V. *J. Chem. Soc., Dalton Trans.* **1990**, 2213. (g) Yamada, K.; Fukuda, Y.; Kawamoto, T.; Kushi, Y.; Mori, W.; Unuora, K. *Bull. Chem. Soc. Jpn.* **1993**, *66*, 2758. (h) Escuer, A.; Vicente, R.; Ribas, J.; Jaud, J.; Raynaud, B. *Inorg. Chim. Acta* **1994**, *216*, 139.
(7) (a) Cavid, S. *Bull. Soc. Fr. Mineral. Crystallogr.* **1959**, *82*, 50. (b) Wrobleski, J. T.; Brown, D. B. *Inorg. Chem.* **1979**, *18*, 498. (c) Julve, M.; Kahn, O. *Inorg. Chim. Acta* **1983**, *76*, L39. (d) Lloret, F.; Julve, M.; Faus, J.; Solans, X.; Journaux, Y.; Morgenstern-Badarau, I. *Inorg. Chem.* **1990**, *29*, 2232. (e) Decurtins, S.; Schmalle, H. W.; Schneuwly, P.; Oswald, H. R. *Inorg. Chem.* **1993**, *32*, 1888. (f) Mathonière, C.; Carling, S. G. Yusheng, D.; Day, P. *J. Chem. Soc., Chem. Commun.* **1994**, 1551.
(8) (a) Verdaguer, M. Ph. D. Thesis, University of Paris-Sud, Orsay, 1984. (b) Wieghardt, K.; Bossek, U.; Nuber, B.; Weiss, J.; Bonvoisin, J.; Corbella, M.; Vitols, S. E.; Girerd, J. J. *J. Am. Chem. Soc.* **1988**, *110*, 7398. (c) Deguenon, D.; Bernardelli, G.; Tuchagues, J. P.; Castan, P. *Inorg. Chem.* **1990**, *29*, 3031. (d) De Munno, Ruiz, R.; Lloret, F.; Faus, J.; Sessoli, R.; Julve, M. *Inorg. Chem.* **1995**, *34*, 408.
(9) Kahn, M. I.; Chang, Y. D.; Chen, Q.; Salta, J.; Lee, Y. S.; O'Connor, C. J.; Zubieta, J. *Inorg. Chem.* **1994**, *33*, 6340.
(10) (a) Verdaguer, M.; Julve, M.; Michalowicz, A.; Kahn, O. *Inorg. Chem.* **1983**, *22*, 2624. (b) Julve, M.; Verdaguer, M.; Charlot, M. F.; Claude, R. *Inorg. Chim. Acta* **1984**, *82*, 5. (c) Pei, Y.; Journaux, Y.; Kahn, O. *Inorg. Chem.* **1989**, *28*, 100. (d) Tamaki, H.; Zhong, Z. J.; Matsumoto, N.; Kida, S.; Koikawa, M.; Achiwa,.N.; Hashimoto, Y.; Okawa, H. *J. Am. Chem. Soc.* **1992**, *114*, 6974. (e) Ohba, M.; Tamaki, H.; Matsumoto, N.; Okawa, H. *Inorg. Chem.* **1993**, *32*, 5385. (f) Decurtins, S.; Schmalle, H. W.; Oswald, H. R.; Linden, A.; Ensling, J.; Gütlich, P.; Hauser, A. *Inorg. Chim. Acta* **1994**, *216*, 65. (g) Cortés, R.; Urtiaga, M. K.; Lezama, L.; Arriortua, M. I.; Rojo, T. *Inorg. Chim. Acta* **1994**, *33*, 829. (h) Van Kralingen, C. G.; Van Ooijen, J. A. C.; Reedijk, J. *Transition Met. Chem. (Weinheim, Ger.)* **1978**, *3*, 90.

S0020-1669(95)01081-0 CCC: $12.00

make it very easy to investigate the influence of the symmetry of the magnetic orbital in the oxalato-bridged dinuclear copper(II) complexes. Recently, some of us have tuned the exchange coupling J between -13 and -386 cm^{-1} in the family of complexes of formula $[Cu_2(bipy)_2(ox)]X_2$ where the end-cap ligand bipy (bipy = 2,2′-bipyridine) is kept and only the nature of the counterion (X) is changed.[11] It was also shown how this range of values can be finely tuned up to -800 cm^{-1} by substituting the oxalate-oxygen atoms by less electronegative atoms such as nitrogen (oxamato and oxamidato),[12] nitrogen and sulfur (dithiooxamidato)[13] and sulfur (tetrathiooxalato).[14]

A careful revision of the available magnetostructural information dealing with oxalato- and oxalato-type-bridged dinuclear complexes reveals that the nature of the peripheral donor atoms also exerts a significant role on the magnitude of the exchange coupling. The present contribution is devoted to the analysis of this factor which was previously unexplored. To do that, we have focused on oxalato-bridged nickel(II) complexes where the metal ion is six-coordinated. The reason of this choice is to fix the symmetry of the interacting magnetic orbitals (d_{xy} and d_{z^2} in the case of Ni(II)), avoiding thus the possibility that symmetry changes of the magnetic orbitals which are often associated with a change of chromophore in the case of other metal ions such as copper(II) could mask the proposed analysis. In the present work,we report first the preparation and structural and magnetic characterization of two oxalato-bridged nickel(II) dimers of formula $(H_3dien)_2[Ni_2(ox)_5]\cdot 12H_2O$ (**1**) and $[Ni_2(dien)_2(H_2O)_2(ox)]Cl_2$ (**2**) (dien = diethylenetriamine). The presence of terminal oxalate (**1**) and tridentate dien in the *fac*-conformation (**2**) is observed for the first time in the coordination chemistry of Ni(II). Second, the variation of $-J$ between 22 and 39 cm^{-1} in oxalato-bridged nickel(II) dimers, the metal chromophore being NiN_pO_q ($p + q = 6$ with $p = 4-0$ and $q = 6-2$), is rationalized on the basis of theoretical calculations. Finally, the results of this investigation are successfully extended to parent bischelating ligands.

Experimental Section

Materials. Diethylenetriamine, nickel(II) chloride hexahydrate, and potassium oxalate monohydrate were Merck reagent grade chemicals and they were used as received. Elemental analyses (C, H, N) were carried out by the Microanalytical Service from the Universidad del País Vasco. Nickel contents were determined by absorption spectrometry.

Synthesis of the Complexes. $(H_3dien)_2[Ni_2(ox)_5]\cdot 12H_2O$ (1). Nickel(II) chloride hexahydrate (0.694 g, 2.91 mmol) dissolved in water (10 mL) was added dropwise to a stirred aqueous solution (20 mL) of $K_2C_2O_4\cdot H_2O$ (2.000 g, 10.09 mmol). The resulting light green solution became dark green (pH = 5) after the addition of diethylenetriammonium chloride (0.620 g, 2.91 mmol). The mixture was stirred at room temperature for 1 h. A polycrystalline solid was obtained when the mixture was allowed to stand for 2 weeks (yield: 0.454 g, 32% of the theoretical referred to Ni). Light green single-crystals of **1** were obtained by recrystallization in *N*,*N*′-dimethylformamide. They were filtered off, washed with water and ethanol and dried in air. Anal. Calcd for $C_{18}H_{56}N_6Ni_2O_{32}$ (**1**): C, 21.93; H, 5.72; N, 8.52; Ni, 11.90. Found: C, 21.86; H, 5.80; N, 8.59; Ni, 11.85. The number of crystallization water molecules was also determined by thermal decomposition of the compound in argon and argon−oxygen atmospheres.

Table 1. Crystallographic Data for $(H_3dien)_2[Ni_2(ox)_5]\cdot 12H_2O$ (**1**) and $[\{Ni_2(dien)_2(H_2O)_2(ox)]Cl_2$ (**2**)

	1	**2**
formula	$C_{18}H_{56}N_6Ni_2O_{32}$	$C_{10}H_{30}Cl_2N_6Ni_2O_6$
fw	986.04	518.67
cryst syst	orthorhombic	monoclinic
space group	Abnn	$P2_1/c$
a, Å	15.386(4)	10.579(1)
b, Å	15.710(4)	7.258(1)
c, Å	17.071(4)	13.326(1)
β, deg		93.52(3)
V, Å^3	4126(2)	1021.3(2)
Z	4	2
T, °C	23(1)	23(1)
λ, Å	0.710 69	0.710 69
ρ(obsd), g cm^{-3}	1.60(1)	1.69(1)
ρ(calcd), g cm^{-3}	1.59	1.69
μ(Mo Kα), cm^{-1}	10.199	21.536
R,[a] %	4.9	8.1
R_w,[b] %	4.9	9.1

[a] $R = \sum||F_o| - |F_c||/\sum|F_o|$. [b] $R = [w(|F_o| - |F_c|)^2/\sum|F_o|^2]^{1/2}$.

$[Ni_2(dien)_2(H_2O)_2(ox)]Cl_2$ (2). A concentrated aqueous solution of nickel(II) chloride hexahydrate (1.300 g, 5.46 mmol) and dien (1.50 mL, 13.81 mmol) was added dropwise to a green aqueous solution (20 mL) of nickel(II) chloride hexahydrate (1.300 g, 5.46 mmol) and potassium oxalate monohydrate (3.000 g, 16.28 mmol) with continuous stirring. The dark blue solution was filtered and allowed to evaporate at room temperature. Blue crystals of **2** were deposited after a week that were redissolved in hot water in order to obtain single crystals suitable for X-ray analysis. The crystals were collected, washed with cold water, and air-dried. Anal. Calcd for $C_{10}H_{30}Cl_2N_6Ni_2O_6$ (**2**): C, 23.16; H, 5.83; N, 16.20; Ni, 22.63. Found: C, 23.14; H, 5.80; N, 16.29; Ni, 22.70.

Physical Measurements. IR spectra were taken on a Nicolet 740 FTIR spectrophotometer in the 4000−400 cm^{-1} region as KBr pellets. Electronic spectra were recorded on a Perkin-Elmer Lambda 9 spectrometer as Nujol mulls on filter paper. The magnetic susceptibility were measured in the temperature range 4−300 K with a fully automated AZTEC DSM8 pendulum-type susceptometer equipped with a TBT continuous-flow cryostat and a Bruker BE15 electromagnet operating at 1.8 T. Mercury(II) tetrakis(thiocyanato)cobaltate(II) was used as a susceptibility standard. Corrections for the diamagnetism of complexes **1** and **2** were estimated from Pascal constants as -461×10^{-6} and -278×10^{-6} cm^3 mol^{-1}, respectively. Experimental susceptibilities were also corrected for the temperature-independent paramagnetism (-100×10^{-6} cm^3 mol^{-1} per Ni(II)).

Crystallographic Data Collection and Structure Determination. Diffraction data of **1** and **2** were collected on an Enraf-Nonius CAD4 four-circle diffractometer by using graphite-monochromated Mo Kα radiation (λ = 0.710 69 Å) and operating in the $\omega-2\theta$ scan mode. A polyhedral light green single crystal of **1** and a blue plate of **2** of dimensions 0.15 × 0.25 × 0.33 and 0.12 × 0.23 × 0.27 mm^3 respectively, were used for data collection. Cell parameters were determined by least-squares fit of 25 well-centered independent reflections in the range $6 < \theta < 15°$ (**1**) and $6 < \theta < 17°$ (**2**). Details on crystal data, intensity collection, and some features of the structure refinement are summarized in Table 1. A full length table of crystallographic data is given as Supporting Information (Table S1). The intensity of two standard reflections which were measured every hour showed no sign of crystal deterioration. A total of 4516 (**1**) ($0 \le h \le 24$; $0 \le k \le 25$; $0 \le l \le 27$) and 4458 (**2**) ($0 \le h \le 17$; $0 \le k \le 11$; $-21 \le l \le 21$) unique reflections were recorded in the range $2 \le 2\theta \le 70°$; 1141 (**1**) and 1153 (**2**) of them were considered as observed

(11) Julve, M.; Gleizes, A.; Kahn, O.; Verdaguer, M. Manuscript in preparation.
(12) (a) Verdaguer, M.; Kahn, O.; Julve, M.; Gleizes, A. *Nouv. J. Chim.* **1985**, *9*, 325. (b) Journaux, Y.; Sletten, J.; Kahn, O. *Inorg. Chem.* **1985**, *24*, 4063.
(13) (a) Chauvel, C.; Girerd, J. J.; Jeannin, Y.; Kahn, O.; Lavigne, G. *Inorg. Chem.* **1979**, *18*, 3015. (b) Veit, R.; Girerd, J. J.; Kahn, O.; Robert, F.; Jeannin, Y.; El Murr, N. *Inorg. Chem.* **1984**, *23*, 4448. (c) Gleizes, A.; Verdaguer, M. *J. Am. Chem. Soc.* **1984**, *106*, 3727. (d) Veit, R.; Girerd, J. J.; Kahn, O.; Robert, F.; Jeannin, Y. *Inorg. Chem.* **1986**, *25*, 4175. (e) Okawa, H.; Matsumoto, N.; Koikawa, M.; Takeda, K.; Kida, S. *J. Chem. Soc., Dalton Trans.* **1990**, 1383. (f) Mitsumi, M.; Okawa, H.; Sakiyama, H.; Ohba, M.; Matsumoto, N.; Kurisaki, T.; Wakita, H. *J. Chem. Soc., Dalton Trans.* **1993**, 2991.
(14) Vicente, R.; Ribas, J.; Alvarez, S.; Seguí, A.; Solans, X.; Verdaguer, M. *Inorg. Chem.* **1987**, *26*, 4004.

Table 2. Fractional Atomic Coordinates and Equivalent Isotropic Thermal Parameters (Å^2 × 10^3; Å^2 × 10^4 for Ni atom) for Compound **1**

atom	*x*/*a*	*y*/*b*	*z*/*c*	U_{eq}[a]
Ni(1)	0.2500	0.2500	0.1576(1)	303(5)
O(2)	0.2442(4)	0.1647(2)	0.0652(2)	37(1)
O(3)	0.2606(4)	0.1566(3)	0.2398(3)	59(2)
O(4)	0.3819(2)	0.2410(3)	0.1603(2)	41(1)
C(2)	0.2500	0.2009(3)	0.0000	27(2)
C(3)	0.3387(5)	0.1372(5)	0.2534(5)	66(3)
C(4)	0.4083(4)	0.1814(4)	0.2030(4)	48(2)
O(31)	0.3659(4)	0.0862(5)	0.3042(5)	129(3)
O(41)	0.4844(3)	0.1555(3)	0.2062(4)	64(2)
N(10)	0.0118(5)	0.1224(4)	0.1075(5)	62(2)
C(11)	0.0571(6)	0.0395(5)	0.1064(6)	75(3)
C(12)	0.1071(5)	0.0201(5)	0.1805(6)	73(3)
N(13)	0.0522(5)	0.0000	0.2500	60(3)
O(5)$_w$	0.1678(9)	0.4900(7)	0.0714(6)	208(7)
O(6)$_w$	0.5455(8)	0.1637(6)	0.0419(5)	150(5)
O(7)$_w$	0.737(2)	0.142(2)	0.042(1)	189(10)[b]
O(8)$_w$	0.655(2)	0.225(2)	0.121(2)	205(11)[b]

[a] $U_{eq} = (1/3)\sum[\mathbf{U}_{ij}\cdot a_i^*\cdot a_j^*\cdot a_i\cdot a_j\cdot\cos(a_i,a_j)]$. [b] Atoms refined isotropically with occupancy factors of 0.5.

by applying the conditions $I \geq 2\sigma(I)$ (**1**) and $I \geq 3\sigma(I)$ (**2**). Data were corrected for Lorentz and polarization effects. An empirical absorption correction, following the procedure DIFABS[15] with minimum and maximum correction coefficients of 0.853 and 1.286 (**1**) and 0.786 and 1.294 (**2**), was applied.

The structures of **1** and **2** were solved by combination of Patterson and difference Fourier methods and refined by full-matrix least-squares methods. In both cases, all non-hydrogen atoms were refined anisotropically except two water molecules of compound **1**, which appear to be disordered with respect to a 2-fold axis and were isotropically refined with an occupancy factor of 0.5. Hydrogen atoms were included at geometrical positions and refined as fixed contributors ($U = 0.05$ Å^2), except for the hydrogen atoms of the protonated amine groups of compound **1** which were refined isotropically because they were clearly visible in a difference-Fourier synthesis. After the final refinement cycle, the agreement factors were $R(F_o) = 0.049$ and $R_w(F_o) = 0.049$, 148 variables, $S = 1.09$, $(\Delta/\sigma)_{max} = 0.44$, $(\Delta/\sigma)_{av} = 0.04$, and $\Delta\rho_{max} = 0.58$ e Å^{-3} for compound **1**, and $R(F_o) = 0.081$ and $R_w(F_o) = 0.091$, 118 variables, $S = 1.29$, $(\Delta/\sigma)_{max} = 0.021$, $(\Delta/\sigma)_{av} = 0.003$, and $\Delta\rho_{max} = 1.64$ e Å^{-3}, for compound **2**. The atomic scattering factors and anomalous dispersion factors were taken from ref 16. Most calculations were carried out by using the X-RAY76 System.[17] Graphical manipulations were produced by the ORTEP program.[18] The final atomic positional parameters for the non-hydrogen atoms are listed in Tables 2 (**1**) and 3 (**2**) whereas the selected bond distances and angles are listed in Tables 4 (**1**) and 5 (**2**). Anisotropic temperature factors (Tables S2 and S3), hydrogen atom coordinates (Tables S4 and S5), nonessential bond lengths and angles (Tables S6 and S7), hydrogen bonds (Tables S8 and S9) and least-squares planes (Tables S10 and S11) are available as Supporting Information.

Results and Discussion

Description of the Structures. $(H_3dien)_2[Ni_2(ox)_5]\cdot 12H_2O$ (1). The crystal structure of **1** is built up by dinuclear $[Ni_2(ox)_5]^{6-}$ anions (Figure 1), axiosymmetric diethylenetriammonium $(H_3dien)^{3+}$ cations, and crystallization water molecules linked together by means of electrostatic interactions and an extensive network of hydrogen bonds. Two nickel(II) ions and five oxalate groups form a dimeric complex in which each metal atom is coordinated to three oxalate groups, two of them being bidentate and adopting a *cis*-arrangement and the third one being bischelating. Thus, each nickel atom shows a distorted NiO_6 octahedral environment with the O(2) and O(2)^i (i = $-x + {}^1/_2$, $-y + {}^1/_2$, z) oxygens of the oxalato bridge and the O(3) and O(3)^i oxygens of the two terminal oxalates building the equatorial plane whereas the apical positions are filled by the O(4) and O(4)^i oxygens atoms. As far as we are aware, **1** is the first crystallographically characterized oxalate-containing nickel(II) complex in which the metal atom is bound to three oxalate ligands.

The dinuclear complex unit has a D_2 point symmetry, the nickel atoms being in a 2-fold axis which is perpendicular to the C(2)−C(2)^i bond of the oxalate bridge. This axis relates the two terminal oxalate ligands and bisects the O(2)−Ni−O(2)^i and O(3)−Ni−O(3)^i bond angles. The halves of the dinuclear unit are related by two perpendicular 2-fold axes which pass through the midpoint of the oxalato C(2)−C(2)^i bond. The Ni−O bond distance [2.072(4) Å] and the O−Ni−O^i bond angle [80.8(1)°] in the five-membered rings of the bis(bidentate) oxalate are very close to the reported ones for other oxalato-

Table 3. Fractional Atomic Coordinates and Equivalent Isotropic Thermal Parameters (Å^2 × 10^3; Å^2 × 10^4 for Ni atom) for Compound **2**

atom	*x*/*a*	*y*/*b*	*z*/*c*	U_{eq}[a]
Ni(1)	0.1251(2)	0.2668(2)	0.1343(1)	155(3)
Cl	0.7125(4)	0.0942(6)	0.6268(3)	36(1)
O(1)	0.0598(9)	0.5414(15)	0.1232(6)	22(3)
O(2)	0.0368(9)	0.2660(15)	−0.0133(6)	24(2)
C(11)	0.0068(11)	0.5848(18)	0.0382(8)	16(3)
N(1)	0.188(1)	−0.003(2)	0.119(1)	31(4)
C(2)	0.288(2)	0.000(3)	0.047(1)	44(6)
C(3)	0.372(2)	0.160(3)	0.077(2)	43(6)
N(4)	0.306(1)	0.340(2)	0.089(1)	27(3)
C(5)	0.358(1)	0.462(2)	0.168(1)	30(4)
C(6)	0.340(2)	0.387(3)	0.272(1)	43(6)
N(7)	0.209(1)	0.322(2)	0.280(1)	25(3)
O(3)$_w$	−0.048(1)	0.179(2)	0.188(1)	28(3)

[a] $U_{eq} = (1/3)\sum[\mathbf{U}_{ij}\cdot a_i^*\cdot a_j^*\cdot a_i\cdot a_j\cdot\cos(a_i,a_j)]$.

Table 4. Selected Bond Distances (Å) and Angles (deg) for Compound **1**[a]

Nickel(II) Coordination Sphere			
Ni(1)−O(2)	2.072(4)	Ni(1)−O(4)	2.035(3)
Ni(1)−O(3)	2.037(5)		
O(2)−Ni(1)−O(2)^i	80.8(1)	O(3)−Ni(1)−O(4)	81.6(2)
O(2)−Ni(1)−O(3)	93.6(1)	O(3)−Ni(1)−O(3)^i	92.9(2)
O(2)−Ni(1)−O(4)	90.9(2)	O(3)−Ni(1)−O(4)^i	96.6(2)
O(2)−Ni(1)−O(3)^i	170.8(2)	O(4)−Ni(1)−O(4)^i	177.4(2)
O(2)−Ni(1)−O(4)^i	91.1(2)		
Oxalate Ligands			
C(2)−O(2)	1.253(4)	C(3)−C(4)	1.540(10)
C(2)−O(2)^{ii}	1.252(4)	C(3)−O(31)	1.252(12)
C(2)−C(2)^i	1.543(7)	C(4)−O(4)	1.254(8)
C(3)−O(3)	1.261(9)	C(4)−O(41)	1.239(8)
O(2)−C(2)−C(2)^i	117.0(2)	O(31)−C(3)−C(4)	116.3(6)
O(2)−C(2)−O(2)^{ii}	126.0(4)	O(4)−C(4)−C(3)	115.8(5)
C(2)^i−C(2)−O(2)^{ii}	117.0(2)	O(4)−C(4)−O(41)	125.3(6)
O(3)−C(3)−O(31)	126.9(8)	O(41)−C(4)−C(3)	118.6(2)
O(3)−C(3)−C(4)	116.8(7)		
Diethylenetriamonium Cation			
N(10)−C(11)	1.478(10)	C(11)−C(12)	1.512(13)
N(13)−C(12)	1.490(10)		
N(10)−C(11)−C(12)	114.0(7)	C(12)−N(13)−C(12)^{iii}	110.9(6)
C(11)−C(12)−N(13)	114.8(6)		

[a] Symmetry code: (i) $-x + {}^1/_2$, $-y + {}^1/_2$, z; (ii) $-x + {}^1/_2$, y, $-z$; (iii) x, $-y$, $-z + {}^1/_2$.

(15) Walker, N.; Stuart, D. *Acta Crystallogr.* **1983**, *A39*, 158.
(16) *International Tables for X−ray Crystallography*; Kynoch: Birmingham, England, 1974; Vol. IV.
(17) Stewart, J. M.; Machin, P. A.; Dickinson, C. W.; Ammon, H. L.; Heck, H.; Flack, H. *The X-RAY76 System*; Technical Report TR-446; Computer Science Center, University of Maryland: College Park, MD, 1976.
(18) Johnson, C. K. *ORTEP*; Report ORNL-3794; Oak Ridge National Laboratory: Oak Ridge, TN, 1965.

Table 5. Selected Bond Distances (Å) and Angles (deg) for Compound **2**[a]

Nickel(II) Coordination Sphere			
Ni(1)−O(3)$_w$	2.10(1)	Ni(1)−N(1)	2.08(1)
Ni(1)−O(1)	2.11(1)	Ni(1)−N(4)	2.11(1)
Ni(1)−O(2)	2.13(1)	Ni(1)−N(7)	2.12(1)
O(3)$_w$−Ni(1)−N(1)	92.2(5)	O(1)−Ni(1)−N(7)	90.3(4)
O(3)$_w$−Ni(1)−N(4)	175.4(5)	O(1)−Ni(1)−O(2)	79.3(4)
O(3)$_w$−Ni(1)−N(7)	94.3(4)	O(1)−Ni(1)−N(1)	170.4(5)
O(3)$_w$−Ni(1)−O(1)	91.2(4)	O(1)−Ni(1)−N(4)	92.4(5)
O(3)$_w$−Ni(1)−O(2)	88.2(4)	O(2)−Ni(1)−N(1)	91.8(5)
N(1)−Ni(1)−N(4)	84.7(5)	O(2)−Ni(1)−N(4)	95.2(5)
N(1)−Ni(1)−N(7)	98.4(5)	O(2)−Ni(1)−N(7)	169.3(5)
N(4)−Ni(1)−N(7)	82.9(5)		
Oxalate Ligand			
C(11)−O(1)	1.27(1)	C(11)−C(11)^i	1.60(2)
C(11)^i−O(2)	1.21(2)		
Ni(1)−O(1)−C(11)	115(1)	O(2)−C(11)^i−O(2)^i	145(1)
Ni(1)−O(2)−C(11)^i	113(1)	O(1)−C(11)−C(11)^i	113(1)
O(1)−C(11)−O(1)^i	142(1)	O(2)−C(11)^i−C(11)	120(1)
Diethylenetriamine Ligand			
C(2)−N(1)	1.48(3)	C(5)−N(4)	1.46(2)
C(2)−C(3)	1.50(3)	C(5)−C(6)	1.51(3)
C(3)−N(4)	1.50(3)	C(6)−N(7)	1.47(2)
N(1)−C(2)−C(3)	106(2)	Ni(1)−N(1)−C(2)	107(1)
C(2)−C(3)−N(4)	115(1)	Ni(1)−N(4)−C(3)	105(1)
C(3)−N(4)−C(5)	117(1)	Ni(1)−N(4)−C(5)	104.9(9)
N(4)−C(5)−C(6)	112(1)	Ni(1)−N(7)−C(6)	110.0(9)
C(5)−C(6)−N(7)	111(1)		

[a] Symmetry code: (i) $-x, -y + 1, -z$.

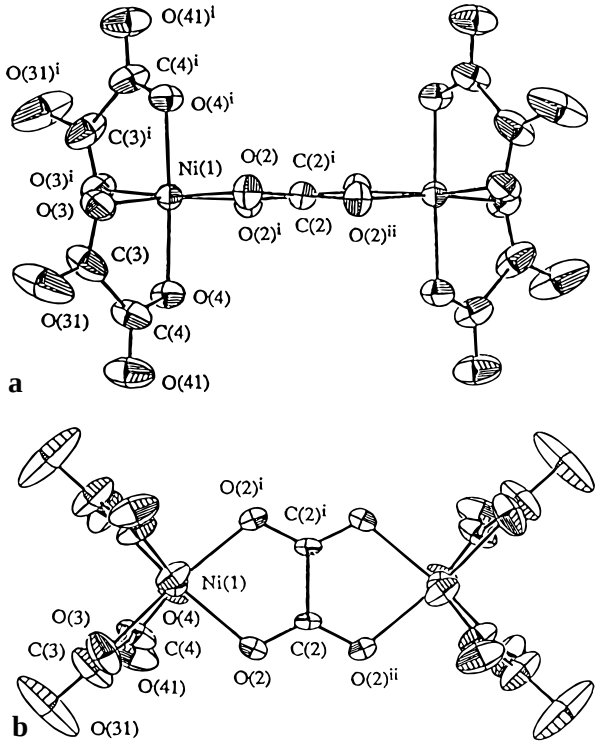

Figure 1. ORTEP drawing of the $[Ni_2(ox)_5]^{6-}$ dinuclear entity of compound **1** showing the atom-labeling scheme: (a) side view to illustrate the planarity of the central Ni(ox)Ni unit; (b) top view to show the planarity of the peripheral oxalato ligands. Thermal ellipsoids are drawn at the 30% probability level.

bridged nickel(II) binuclear complexes,[19] but they are slightly different to those involving the terminal oxalates [2.035(3) and 2.037(5) Å; 81.6(2)°]. These last values are comparable with those found for bidentate oxalate ligands in mononuclear octahedral nickel(II) complexes.[20] It deserves to be noted that square planar oxalato-bridged nickel(II) complexes such as $\{Ni_2(CH_3)_2[P(CH_3)_3](ox)\}$[21] exhibit significantly shorter Ni−O(oxalate) bonds (1.990(3) and 1.961(3) Å) and larger O−Ni−O(oxalate) angles (84.3(1)°) as expected. Bond distances and angles within the bridging and terminal oxalate groups are similar and they are in the range observed in other oxalate-containing nickel(II) complexes. However, two important unusual features are observed in **1** when regarding the structure of the oxalato bridge: first, it has a D_2 point symmetry with four identical C−O bonds, which is the higher symmetry found in analogous complexes; and second, it is not planar, the distortion arising form a twisting about the C(2)−C(2)^i bond which leads to a dihedral angle of 9.2(3)° between the O(2), C(2), O(2)^{ii} (ii $= -x + 1/2, y, -z$) and O(2)^i, C(2)^i, O(2)^{iv} (iv $= -x, -y + 1/2, -z$) planes. A similar distortion of 10.1(8)° is also observed in the terminal oxalate ligands. The dissimilar hydrogen bonding interactions involving the oxygen atoms of the oxalate anions are at the origin of this deviation. The intramolecular Ni···Ni separation is 5.380(2) Å whereas the shortest intermolecular Ni···Ni distance is 8.315(2) Å.

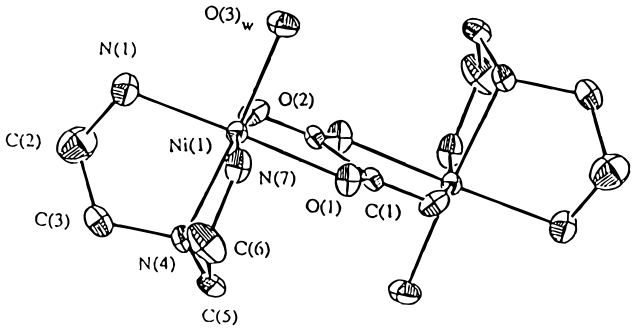

Figure 2. ORTEP drawing of the $[Ni_2(dien)_2(H_2O)_2(ox)]^{2+}$ dinuclear entity of compound **2** showing the atom-labeling scheme. Thermal ellipsoids are drawn at the 30% probability level. Hydrogen atoms have been omitted for the sake of clarity.

As far as the diethylenetriammonium cation is concerned, it is axiosymmetric with respect to the central nitrogen atom and the dihedral angles along the chain indicate a *gauche* (72°)−*trans* (178°) conformation. Its bond lengths and bond angles are comparable to those previously reported for this cation.[22] A hydrogen-bonding pattern involving lattice water molecules, organic cations, and oxalate oxygen atoms (N···O(ox) and O$_w$···O(ox) being comprised in the ranges 2.760−3.303 and 2.785−2.963 Å, respectively),[23] ensures the cohesion of the crystal lattice.

$[Ni_2(dien)_2(H_2O)_2(ox)]Cl_2$ (2). The structure of this compound consists of noncoordinated chloride ions and $[Ni_2(dien)_2(H_2O)_2(ox)]^{2+}$ dinuclear cations (Figure 2) having a symmetry center at the midpoint of the C(1)−C(1)^i (i $= -x, -y + 1, -z$) bond of the oxalato bridge. The oxalate ion joins two adjacent coordination polyhedra with its oxygen atoms occupying in both polyhedra two cis positions, and the dien group acts as a facially coordinated tridentate ligand.

The coordination geometry around each metal ion is NiN_3O_3 distorted octahedral. The equatorial plane is built by the O(1) and O(2) oxygens from oxalate and N(1) and N(7) nitrogens

(19) (a) Curtis, N. F.; McCormick, I. R. N.; Waters, T. N. *J. Chem. Soc., Dalton Trans.* **1973**, 1537. (b) Davis, A. R.; Einstein, F. W. B.; Willis, A. C. *Acta Crystallogr.* **1982**, *B38*, 443. (c) Alcock, N. W.; Moore, P.; Omar, H. A. A. *Acta Crystallogr.* **1987**, *C43*, 2074.

(20) Román, P.; Guzmán-Miralles, C.; Luque, A. *Acta Crystallogr.* **1993**, *C49*, 1336.

(21) Klein, H.-F.; Wiemer, T.; Menu, M.-J.; Dartiguenave, M.; Dartiguenave, Y. *Inorg. Chim. Acta* **1988**, *154*, 21.

(22) Román, P.; Luque, A.; Aranzabe, A.; Gutiérrez-Zorrilla, J. M. *Polyhedron* **1992**, *11*, 2027.

(23) (a) Taylor, R.; Kennard, O. *Acc. Chem. Res.* **1984**, *17*, 320. (b) Desiraju, G. R. *Acc. Chem. Res.* **1991**, *24*, 290.

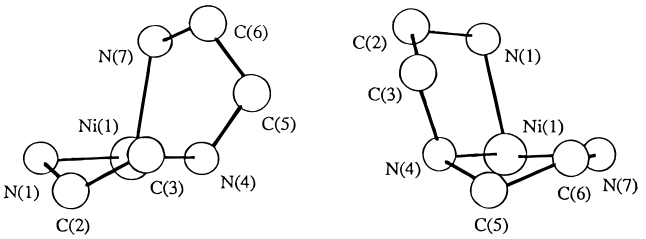

Figure 3. Ball and stick drawing of the two Ni−dien chelate rings in **2**. The N−Ni−N planes have been drawn perpendicular to the plane of the sheet in order to assign the chirality through IUPAC rules.

from dien, whereas the axial positions are occupied by a $O(3)_w$ water molecule and the remaining N(4) atom from dien. The values of the Ni−N bond lengths are in the range 2.08−2.12 Å and are comparable with those reported in the literature for other nickel(II) complexes with *fac*-coordinated 1,4,7-triazacyclononane[6f,24] and its N-methylated derivative.[25] The Ni−O(ox) bonds are within a narrow range [2.11−2.13 Å] and they are somewhat longer than that found in compound **1**. The Ni−$O(3)_w$ axial bond is almost perpendicular [86.85°] to the mean O(1)−O(2)−N(1)−N(7) equatorial plane. The metal atom is displaced by 0.059(2) Å from this plane. The bridging oxalato is exactly planar, and the nickel(II) ion is 0.072(2) Å out of this plane. The dihedral angle between the equatorial and oxalato mean planes is 4.6(3)°. The O(1)−Ni(1)−O(2) angle is 79.3(4)°, a value very close to the related one observed in **1**.

Bond distances and angles of the *fac*-coordinated dien ligand are close to those found in H_3dien^{3+} in **1** and in other dien−containing metal complexes.[26] The conformation of the two rings of dien can be analyzed in terms of the distances of the carbon atoms from the N−Ni−N plane. Distances from C(2) and C(3) to the N(1)−Ni(1)−N(4) plane are −0.59(2) and +0.04(2) Å, respectively. Distances from C(5) and C(6) to the N(4)−Ni(1)−N(7) plane are −0.62(2) and −0.07(2) Å, respectively. The two rings show an asymmetric distribution of the carbon atoms, but whereas they are above and below the plane in the first one, they are located on the same side of the plane in the second one. The two chelate rings adopt the λ conformation as shown in Figure 3. Dien-containing metal complexes have been widely investigated,[27] and although both *mer*- and *fac*-M(dien)$(XYZ)^{n+}$ complexes for octahedral metal centers can be formed, in general the *mer*-conformer is the more commonly found. The occurrence of the *fac*-conformer has been structurally characterized only in a few cobalt, chromium, molybdenum, and platinum complexes of formulas $[Co(dien)(CN)_3]$,[27c] $[Cr(dien)(CO)_3]$,[27d] $[Mo(dien)(CO)_3]$,[27e] and $[Pt(dien)Cl_3]Cl$.[27f]

The Cl^- anion contributes to the packing by forming hydrogen bonds involving the oxygen atom of the water molecule and the N(4) atom of the diethylenetriamine ligand [3.09(1) Å and 180° for $O(3)_w\cdots Cl^{ii}$ and $O(3)_w-H(32)_w\cdots Cl^{ii}$, respectively; (ii) $x-1, -y+{}^1/_2, z-{}^1/_2$]. The intramolecular Ni···Ni distance is 5.487(2) Å whereas the shortest intermolecular Ni···Ni separation is 5.538(3) Å. This last value, which is significantly shorter than that found in **1**, is due to the more effective packing caused by the smaller net charge and smaller counterion size in **2** with respect to **1**.

Electronic and IR Spectra. The reflectance spectra of compounds **1**, **2** and $[Ni_2(dien)_2(H_2O)_2(ox)](ClO_4)_2$ (**3**)[28] are as expected for a d^8 configuration in a near-octahedral ligand field. The three spin-allowed transitions from $^3A_{2g}$ to $^3T_{2g}$, $^3T_{1g}$ (F) and $^3T_{1g}$ (P) are located at 9100, 14900, and 26700 cm^{-1} for **1**, at 10300, 17500, and 28500 cm^{-1} for **2** and at 10100, 16800, and 26800 cm^{-1} for **3**. The first transition yields the octahedral splitting parameter, 10*Dq*. It can be seen that the substitution of oxygen atoms by nitrogen ones when going from **1** to **2** causes an increase of 10*Dq* as expected. Significant differences are observed in the other two transitions when comparing **2** and **3** although the metal ion has the same chromophore. This fact suggests that these compounds could correspond to isomeric forms, the dien ligand adopting *fac*- (**2**) and *mer*- conformations (**3**). This assumption is also supported by IR data. At this regards, it is known that infrared spectroscopy is a useful tool to distinguish between the *mer*- and *fac*-conformation of dien in its metal complexes.[27g,h] So, the bending mode of methylene group of dien in the *mer*-conformation appears as an assymetrical doublet at 1450 cm^{-1}, whereas the *fac*-one exhibits a clear triplet in the same region which is specific for the *fac*-isomer. The presence of three $\delta(CH_2)$ bands at 1480 w, 1451 m, and 1400 w cm^{-1} for **2** strongly supports the ocurrence of *fac*-dien in this complex, in agreement with its X-ray structure. Only a medium intensity absorption at 1462 cm^{-1} with a week shoulder at 1439 cm^{-1} is observed for complex **3**, pointing out the occurrence of the *mer*-conformation of dien in it. Although the crystal structure of this complex could not be determined, the magnetic properties of **2** and **3** are also consistent with these isomeric forms (*vide infra*).

The IR spectra of **2** and **3** exhibit the characteristic features of the bischelating oxalate:[29] ν_{as}(O−C−O) at 1647 vs (**2**) and 1656 vs (**3**) cm^{-1}, ν_s(O−C−O) at 1356 s and 1316 s cm^{-1} (**2**) and 1360 m and 1316 s cm^{-1} (**3**) and δ(O−C−O) at 806 (**2**) and 800 s (**3**) cm^{-1}. The occurrence of both chelating and bischelating oxalate in **1** is clearly observed in the stretching and deformation vibrations of oxalate: ν_{as}(O−C−O) at 1720 sh and 1630 s cm^{-1}, ν_s(O−C−O) at 1440 s and 1305 s cm^{-1}, and δ(O−C−O) at 795 s cm^{-1} attributed to chelating oxalate whereas ν_{as}(O−C−O) at 1650 s, ν_s(O−C−O) at 1350 m, and δ(O−C−O) at 810 m cm^{-1} were attributed to bischelating oxalate.[29,30] This spectroscopic evidence was proved to be useful to detect the occurrence of both coordination modes of oxalate in oxalato(2,2′-bipyridyl)copper(II) complexes.[5f]

Magnetic Properties. The thermal dependence of the molar magnetic susceptibilty, χ_M, of complexes **1**−**3** (Figure 4) is characteristic of an antiferromagnetic interaction between the two single-ion triplet states: the value of χ_M at room temperature is in the range expected for two $S = 1$ states (μ_{eff} *ca.* 4 μ_β for **1**−**3**), increases as the temperature is lowered until a maximum is reached (T_{max} = 33, 42 and 36 K, for **1**−**3**, respectively), and finally decreases very quickly. The ground state of a nickel(II) ion in an octahedral environment is orbitally nondegenerate, and as such, it is possible to represent the intradimer magnetic

(24) Zompa, L. J.; Margulis, T. N. *Inorg. Chim. Acta* **1978**, *28*, L157.
(25) (a) Chaudhuri, P.; Guttman, M.; Ventur, D.; Wieghardt, K.; Nuber, B.; Weiss, J. *J. Chem. Soc., Chem. Commun.* **1985**, 1618. (b) Chaudhuri, P.; Kuppers, H. J.; Wieghardt, K.; Gehring, S.; Nuber, B.; Weiss, J. *J. Chem. Soc., Dalton Trans.* **1988**, 1367.
(26) Britten, J. F.; Lock, C. J. L. *Acta Crystallogr.* **1980**, *B36*, 2958 and references therein.
(27) (a) House, D. A. In *Comprehensive Coordination Chemistry*, Wilkinson, G.; Gillard, R. D.; McCleverty, J. A., Eds.; Pergamon Press: New York, 1987; Vol. 2, p 23. (b) Vilas, L. F.; Gillard, R. D. G.; Mitchell, P. R. *J. Chem. Soc., Dalton Trans.* **1977**, 1215. (c) Kuroya, H. *Nippon Kagaku Zasshi* **1971**, *92*, 905. (d) Cotton, F. A.; Richardson, D. C. *Inorg. Chem.* **1966**, *5*, 1851. (e) Cotton, F. A.; Wing, R. M. *Inorg. Chem.* **1965**, *4*, 1851. (f) Britten, J. F.; Lock, C. J. L. *Acta Crystallogr.* **1980**, *B36*, 2958. (g) Schmidtke, H. H.; Garthoff, D. *Inorg. Chim. Acta* **1968**, *2*, 357. (h) Gainsford, A. R.; House, D. A. *Inorg. Chim. Acta* **1969**, *3*, 367.
(28) We have synthesized this compound after ref 5a and reinvestigated its spectroscopic and magnetic properties for comparative purposes with its parent compound **2**.
(29) (a) Curtis, N. F. *J. Chem. Soc.* **1963**, 4109. (b) Curtis, N. F. *J. Chem. Soc. A* **1968**, 1584.
(30) Fujita, J.; Martell, A. E.; Nakamoto, K. *J. Chem. Phys.* **1962**, *36*, 324 and references therein.

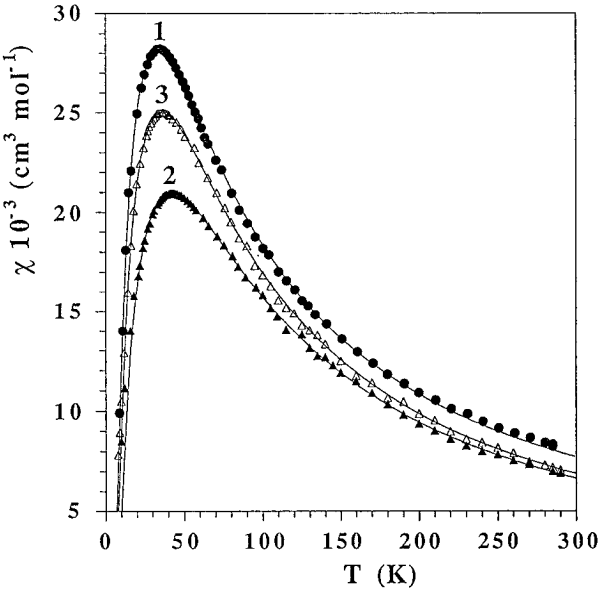

Figure 4. Thermal dependence of the molar magnetic susceptibility for compounds **1**−**3**: (○ (**1**), △ (**2**), △ (**3**)) experimental data; (—) best theoretical fit (see text).

interaction, J, with the isotropic spin hamiltonian $H = -JS_A \cdot S_B$. The molar magnetic susceptibility for a nickel(II) dimer (local spins $S_A = S_B = 1$) may be expressed by eq 1, where N, β, K,

$$\chi_M = \frac{2N\beta^2 g^2}{kT} \times \frac{\exp(J/kT) + 5\exp(3J/kT)}{1 + 3\exp(J/kT) + 5\exp(3J/kT)} \quad (1)$$

g and T have their usual meanings and it is assumed that $g_x = g_y = g_z = g$. Although, nickel(II) in axial symmetry can have a large zero-field splitting, D, the magnetic behavior of nickel(II) dimers closely follows eq 1 when a relatively strong antiferromagnetic interaction is operative ($|J| \geq 20$ cm^{-1}).[31] If the antiferromagnetic coupling is weak or the coupling is ferromagnetic, the influence of D must be taken into account to describe the magnetic behavior at low temperatures.[31] The occurrence of a relatively large intradimer antiferromagnetic coupling in **1**−**3** makes unnecessary the consideration of D, and a good fit of the experimental data to eq 1 is obtained. The best-fit parameters J, g, and R are −22.8 cm^{-1}, 2.15, and 5.1 × 10^{-5} for **1**, −28.8 cm^{-1}, 2.10, and 6.2 × 10^{-5} for **2** and −24.6 cm^{-1}, 2.12, and 3.2 × 10^{-5} for **3**, respectively. R is the agreement factor defined as $R = \sum[(\chi_M^{obs} - \chi_M^{calc})^2/\sum(\chi_M^{obs})^2]$.

The values of J for these oxalato-bridged nickel(II) dimers are significantly different. From a chemical point of view, complexes **2** and **3** only differ in the nature of the counterion (Cl^- or ClO_4^-). The value of the exchange coupling for complex **3** agrees with that previously reported by Hendrickson *et al.* ($J = -24.4$ cm^{-1}).[5a] Although the structure of complex **3** is unknown (all our attempts to grow single crystals suitable for X-ray diffraction were unsuccessful), its spectroscopic properties support the occurrence of dien in the *mer* conformation in contrast to what occurs in complex **2** where this ligand adopts the *fac* one.

The known oxalato-bridged nickel(II) complexes together with their most relevant magnetostructural data are listed in Table 6. A comparison among the J values of the different oxalato-bridged nickel(II) complexes reveals a so great discrepancy that it cannot be attributed to experimental uncertainties. These nickel(II) complexes exhibit the molecular structure sketched by Scheme 1. The donor atoms from the peripheral ligands are amine-nitrogen (cyclic or open amines) and/or water-oxygen, except for compounds **Ib** and **IIa**, where the oxygen atoms are from oxalate and acetylacetonate, respectively.

For comparative purposes, the nickel(II) chain (**Ia**) can be considered as an oxalato-bridged nickel(II) dimer with $A_1 = A_2 =$ O(water) and $E_1 = E_2 =$ O(oxalate) according to Scheme 1. These oxalate-containing complexes have been classified in five groups after the number of N- and O-donors of the peripheral ligands and their location in axial (A_i) or equatorial (E_i) positions. The features to be pointed out from Table 6 are the following.

(i) A significant increase of the magnitude of the exchange coupling (*ca.* 50%) is observed when comparing the complexes belonging to group **I** (NiO_6 chromophore, average J value of −22 cm^{-1}) with those of group **V** (NiN_4O_2 chromophore, average J value of −36 cm^{-1}). The differences observed between the structural parameters of the two families cannot explain the variation of J. In fact, the metal to ligand bond distances and the deviation of the metal atom from the mean oxalate (h'_{Ni}) and equatorial (h_{Ni}) planes are greater in group **V**, and therefore, they would cause a weaker antiferromagnetic coupling in this family,[3] in contrast to the experimental data. The variation of the J value when going from **I** to **V** might be attributed to the different nature of the donor atoms involved: the replacement of O by N atoms is accompanied by an increase of the antiferromagnetic coupling. In this respect, the compounds in the intermediate situation (groups **II**−**IV**) with only a partial replacement of O by N atoms show values of $-J$ between both limits ($24 < -J < 30$ cm^{-1}).

(ii) A comparison between the groups having identical number of N- and O-donors (groups **III** and **IV**) reveals that complexes of group **III** (only one equatorial N-atom) present a smaller antiferromagnetic coupling than those of group **IV** (two equatorial N-atoms). This suggests that the variation of the value of J is more accentuated when the substitutions involve equatorial positions. In this respect, it is very interesting to compare the different values of J determined for the $[Ni_2(dien)_2(H_2O)_2(ox)]^{2+}$ dinuclear unit as chloride (**2**, $J = -28.8$ cm^{-1}) and perchlorate (**3**, $J = -24.6$ cm^{-1}) salts. In the light of the above mentioned features, dien exhibits the *fac*-conformation in the chloride derivative (two equatorial N) whereas it is expected to adopt the *mer*-conformation in the perchlorate one (one equatorial N) leading thus to a greater antiferromagnetic coupling in the former case.

The complex **IIa** (two N atoms, one axial and one equatorial), which is the only example of group **II**, exhibits an antiferromagnetic coupling practically identical to that of complex **IVb** (three N atoms, two equatorial and one axial), namely −28.6 and −28.8 cm^{-1}, respectively. In principle, one would expect that the complex IIa should present a value of J close to that of group **III**. Both the greater basicity of the acetylacetonate-O with respect to that of the water-O and, especially, the very short Ni−O(acetylacetonate) bond length (1.99 Å) would account for this apparent anomalous result.

It is well-known that structural distortions (specially those involving deviations from the planarity of the metal ion respect to the mean plane of the bridging ligand, h'_M, or equatorial, h_M) can play a key role on the fine tuning of the exchange coupling. Although such distortions cannot be responsible for the observed variations of J when going from the top to the bottom in Table 6, they may cause the variations observed within a group or even in neighboring groups. In this respect, the fact that the complex **IVa** exhibits a value of $-J$ (25.5 cm^{-1}) smaller than that of **IVb** ($-J$ *ca* 28.8 cm^{-1}) but close to those of group **III** should be attributed to the greater rigidity of the small triaza macrocycle (tacn) with respect to the open chain triamine (dien).

(31) De Munno, G.; Julve, M.; Lloret, F.; Derory, A. *J. Chem Soc., Dalton Trans.* **1993**, 1179.

Table 6. Selected Magnetostructural Parameters[a−c] for Oxalato-bridged Octahedral Nickel(II) Complexes (A and E Stand for Axial and Equatorial Donors, Respectively; See Scheme 1)

compound	$-J$	$d_{Ni-O(ox)}$	d_{Ni-Ai}	d_{Ni-Ei}	$d_{Ni\cdots Ni}$[d]	h_{Ni} (h'_{Ni})[e]	ref
I.(A = E = O)							
(**a**) $[Ni(ox)(H_2O)_2]_n$[f]	22.0	2.07[f]	2.07[f]	2.07[f]			10h
(**b**) $(H_3dien)_2[Ni_2(ox)_5]\cdot 12H_2O$	22.8	2.07	2.04	2.04	5.38	0.00 (0.00)	this work
II.(A_1 = E_1= N, A_2 = E_2 = O)							
(**a**) $[Ni_2(acac)_2(tmen)_2(ox)]\cdot 2tce$	28.6	2.07	2.14 (N) 2.00 (O)	2.12 (N) 1.99 (O)	5.36	0.01 (0.03)	6g
III.(A = E_1 = N, E_2 = O)							
(**a**) $[Ni_2(dien)_2(H_2O)_2(ox)](ClO_4)_2$	24.4						5a
(**b**) $[Ni_2(Medpt)_2(H_2O)_2(ox)](ClO_4)_2$	21.6	2.14	2.08	2.13 (N) 2.10 (O)	5.44	0.06 (0.17)	6h
(**c**) $[Ni_2(ept)_2(H_2O)_2(ox)](ClO_4)_2$	25.0						6h
(**d**) $[Ni_2(dpt)_2(H_2O)_2(ox)](ClO_4)_2$	24.7	2.11	2.08	2.07 (N) 2.13 (O)	5.49	0.01 (0.06)	6h
IV.(E = A_1= N, A_2 = O)							
(**a**) $[Ni_2(tacn)_2(H_2O)_2(ox)](NO_3)_2$	25.5	2.10	2.08 (N) 2.12 (O)	2.07	5.44	(0.13)	6f
(**b**) $[Ni_2(dien)_2(H_2O)_2(ox)]Cl_2$	28.8	2.12	2.11 (N) 2.10 (O)	2.10	5.49	0.06 (0.07)	this work
V (A = E = N)							
(**a**) $[Ni_2(nn')_2(ox)](ClO_4)_2$	32.4						6c
(**b**) $[Ni_2(Me_2cyclen)_2(ox)](ClO_4)_2$	34.0	2.10	2.15	2.06	5.47	0.00 (0.02)	6e
(**c**) $[Ni_2(cyclen)_2(ox)](NO_3)_2$	35.0						6e
(**d**) $[Ni_2(trien)_2(ox)](ClO_4)_2$	35.2						6a
(**e**) $[Ni_2(tn)_4(ox)](ClO_4)_2$	36.4	2.12	2.09	2.09	5.48	0.02 (0.07)	6c
(**f**) $[Ni_2(en)_4(ox)](ClO_4)_2$	36.8	2.10	2.10	2.09	5.41	0.03 (0.04)	6b
(**g**) $[Ni_2(cth)_2(ox)](ClO_4)_2$	36.8						6a
(**h**) $[Ni_2(cyclam)_2(ox)](ClO_4)_2$	39.0	2.07	2.10	2.09	5.40	0.01 (0.03)	6d

[a] Abbreviations used: acac = acetylacetonate; tmen = *N*,*N*,*N*′*N*′-tetramethylethylenediamine; tce = 1,1,2,2-tetrachloroethane; Medpt = 3,3′-diamino-*N*-methyldipropylamine; ept = *N*-(2-aminoethyl)-1,3-propanediamine; dpt = bis(3-aminopropyl)amine; tacn = 1,4,7-triazacyclononane; nn′ = *N*,*N*′-quinolinediylethylenediamine; Me_2cyclen = 1,7-dimethyl-1,4,7,10-tetraazacyclododecane; cyclen = 1,7-dimethyl-1,4,7,10-tetraazacyclododecane; trien = triethylenetetramine; tn = 1,3-diaminopropane; en = ethylenediamine; cth = 2,4,4,9,9,11-hexamethyl-1,5,8,12-tetraazacyclotetradecane; cyclam = 1,4,8,11-tetraazacyclotetradecane. [b] J in cm^{-1}. [c] $d_{Ni-O(ox)}$, d_{Ni-Ai}, d_{Ni-Ei}, and $h_{Ni}(h'_{Ni})$ in Å. [d] $d_{Ni\cdots Ni}$, is the metal−metal separation across oxalato. [e] h_{Ni} (h'_{Ni}) is the metal height from the equatorial (oxalate) mean plane. [f] EXAFS data.

Scheme 1

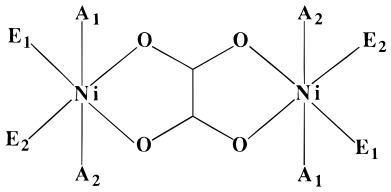

There are geometrical constraints in tacn that cause a deformation of the octahedral surrounding of Ni(II), particulary in the bond angles (greater deviations from the ideal 90° value) and in the planarity of the Ni(ox)Ni fragment (Ni(II) displaced by 0.12 Å from the mean oxalate plane).

It is clear that without the grouping performed in Table 6, the differences in the values of *J* for these oxalato-bridged nickel(II) dimers could appear as meaningless and uncorrelated, and at first sight one might normally be tempted to attribute them to the uncertainty of the experimental measurements and/or the variation of some structural parameters. However, a careful inspection of the data gathered in Table 6 shows a clear trend of the values of *J*, specially when comparing the first and last families (groups **I** and **V**). The variation of structural parameters cannot account for a correct explanation of the *J* values and the nature of the donor atoms of the peripheral ligands appears to be the leading factor, so it cannot be ignored. This phenomenon is not limited to the oxalato-bridged nickel(II) dimers. A review concerning the magnetic properties of polynuclear compounds with oxalato and related bischelating ligands[32] allowed us to generalize such a relevant role of the peripheral ligands on the magnetic properties. Although a thorough review on this type of dimers is not the scope of the present paper, the inclusion of some selected examples which are listed in Table 7 is in order. There, one can see that a decrease of the electronegativity of the peripheral ligand (O, N, Cl, S, Br), keeping the same metal and bridging unit, causes a significant increase of the antiferromagnetic coupling. The variation of *J* as a function of the bridging ligand can be understood taking into account that the efficiency to transmit electronic effects between paramagnetic centers follows the trend dithiooxamidato > oxamidato > oxalato > bipyrimidine.[12a,14]

Although oxamidato-[41] and dithiooxamidato-bridged[13d] nickel(II) dimers are known, they are diamagnetic square planar species due to the greater ligand field strength of these ligands with respect to oxalato. However, an oxamidato-bridged Ni(II) dimer of formula $[Ni_2(glyox)(H_2O)_6]$ has been reported to be paramagnetic.[42] The presence of peripheral carboxylate ligands with a weak ligand field strength (A_1 = A_2 = E_2 = O(water) and E_1 = O(carboxylate) in Scheme 1, the bridging ligand being oxamidate instead of oxalate) and the formation

(32) Verdaguer, M.; Julve, M. *Chem. Rev.*, manuscript in preparation.
(33) Girerd, J. J.; Jeannin, S.; Jeannin, Y.; Kahn, O. *Inorg. Chem.* **1978**, *17*, 3034.
(34) Bencini, A.; Benelli, C.; Fabretti, A. C.; Fanchini, G.; Gatteschi, D. *Inorg. Chem.* **1986**, *25*, 1063.
(35) Lloret, F.; Julve, M.; Faus, J.; Journaux, Y.; Philoche-Levisalles, M.; Jeannin, J. *Inorg. Chem.* **1989**, *28*, 3702.
(36) (a) Julve, M.; De Munno, G.; Bruno, G.; Verdaguer, M. *Inorg. Chem.* **1988**, *27*, 3160. (b) De Munno, G.; Bruno, G. *Acta Crystallogr.* **1984**, *C40*, 2030.
(37) Julve, M.; Verdaguer, M.; De Munno, G.; Real, J. A.; Bruno, G. *Inorg. Chem.* **1993**, *32*, 795.
(38) De Munno, G.; Julve, M.; Lloret, Faus, J.; Canneschi, A. *J. Chem Soc., Dalton Trans.* **1994**, 1175.
(39) Andrés, E.; De Munno, G.; Julve, M.; Real, J. A.; Lloret, F. *J. Chem Soc., Dalton Trans.* **1993**, 2169.
(40) Real, J. A.; Zarembowitch, J.; Kahn, O.; Solans, X. *Inorg. Chem.* **1987**, *26*, 2939.
(41) Ojima, H.; Nonoyama, K. *Coord. Chem. Rev.* **1988**, *92*, 85.
(42) Lloret, F.; Sletten, J.; Ruiz, R.; Julve, M.; Verdaguer, M. *Inorg. Chem.* **1992**, *31*, 778.

Table 7. Peripheral Ligand and Exchange Coupling in Selected Dithiooxamidato-, Oxamidato-, Oxalato-, and 2,2′-Bipyrimidine-bridged Dinuclear Complexes

Dimers with diferent bridging ligand	Peripheral ligand	$-J$ /cm^{-1}	Ref.
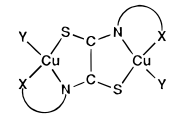	X=Y= O	594	33
	X=S, Y=Cl	650	13b
	X=S, Y=Br	750	13b
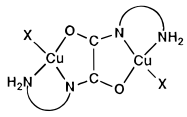	X=O	432	33
	X=N	590	35
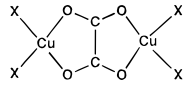	X=O	240	5b
	X=N	385	5c
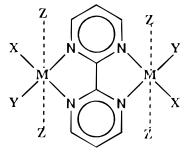	M= Cu(II),		
	X=Y=O	191	36
	X=Y=N	230	37
	M= Co(II),		
	X=Y=Z=O	4.7	38
	X=Y=Z=N	6.2	38
	M= Fe(II),		
	X=Y=Z=O	3.1	39
	X=Y=Z=N	4.1	40

of a very distorted octahedral surrounding around Ni(II) account for this feature. The value of J equal to -25 cm^{-1} for this complex is much more weaker than that expected for an oxamidato-bridged nickel(II) dimer. This lower value was attributed to the distortion of the metal surroundings. However, such a distortion is similar to that showed by complex **IVa** in Table 6, for which a close value of J (-25.5 cm^{-1}) was determined, in spite of the lesser efficieny of oxalato to mediate antiferromagnetic coupling. This situation can be clarified now keeping in mind that the occurrence of peripheral N atoms in the oxalato derivative increases the antiferromagnetic coupling whereas the presence of O atoms in the oxamidato complex decreases it, and so, a very close antiferromagnetic coupling is observed in both compounds.

Unfortunately, the examples gathered in Table 6 present little variations in the nature of the peripheral donor atoms (in general only N or O). This is not unexpected, given that these are the more common donor atoms in coordination chemistry concerning first−row transition metal ions. However, in spite of small electronegativity differences between N and O, their influence on the value of J is significant. Our feeling is that, although the oxalato-bridged dinuclear complexes can be referred to as classical systems in molecular magnetism, the synthesis of new species with different peripheral ligands containing donor atoms other than N or O (for instance P, S, halogens, ...) would be very interesting. They could provide us with a correct estimate of the real influence of the electronegativity of the donor atoms on the magnetic coupling. The polyatomic oxalate-type ligands are the more appropriate bridging group to carry out this study because their rigidity precludes the occurrence of important structural modifications in the dimers. Monoatomic bridges are less suitable due to the unforeseeable variation of the bond angles that they exhibit, which dominates both the magnitude and nature of the magnetic interactions. In the next section, we will try to rationalize the different exchange parameters

Scheme 2

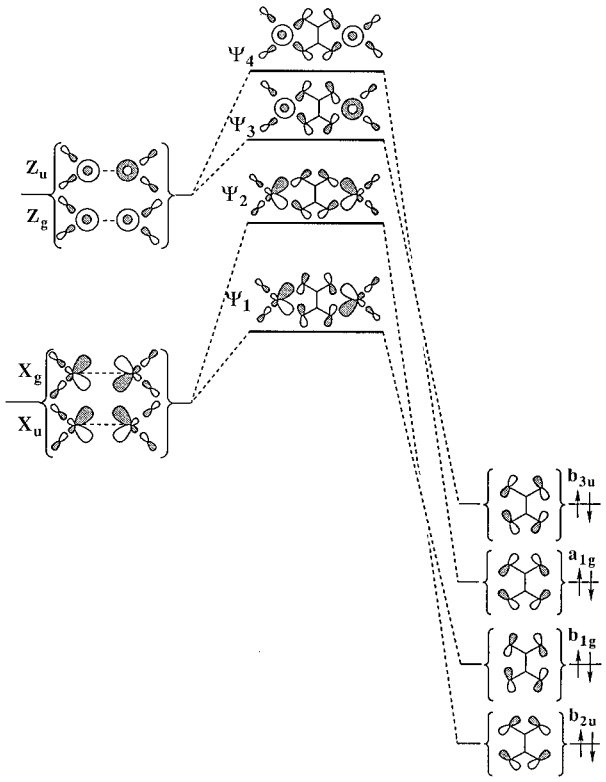

which have been observed through the exploration of the influence of the peripheral ligands.

Role of the Peripheral Ligand: A Molecular Orbital Model. This section is aimed at analyzing and rationalizing the influence of the peripheral ligand on the superexchange interaction by means of a molecular orbital model, using the ideas introduced by Hay, Thibeault, and Hoffmann.[43] These authors showed that, for the coupling of two centers with one electron per center, the singlet−triplet energy separation (J) can be expressed as the sum of ferromagnetic ($J_F > 0$) and antiferromagnetic ($J_{AF} < 0$) contributions. Although two-electron integrals appear in this expression, it is generally accepted[3] that, within a family of related compounds, the two-electron terms are nearly constant and the variations in the values of J are roughly related to the variations in the energy differences between the molecular orbitals bearing the unpaired electrons. Such an approach is in good agreement with the results of more elaborate calculations.[44−46] For the case of octahedral Ni(II) centers, with unpaired electrons in the d_{z^2} and d_{xy} orbitals, this approximation leads to eq 2, where ϵ_i are the energies of the singly-occupied molecular orbitals Ψ_i (SOMO's) represented in Scheme 2 for our model compound (Scheme 1), and k_{ij} represent the supposedly constant two-electron terms.[43]

$$J_{AF} = -{}^1/_2\{k_{12}(\epsilon_2 - \epsilon_1)^2 + k_{34}(\epsilon_4 - \epsilon_3)^2\} \qquad (2)$$

We have calculated the orbital gaps Δ_{xy} ($\epsilon_2 - \epsilon_1$) and Δ_z ($\epsilon_4 - \epsilon_3$) for different combinations of NH_3 and H_2O as peripheral ligands in the dimeric Ni(II) model compound (Scheme 1), by performing extended Hückel (EH) molecular orbital calcula-

(43) Hay, P. J.; Thibeault, J. C.; Hoffmann, R. *J. Am. Chem. Soc.* **1975**, *97*, 4884.
(44) de Loth, P.; Cassoux, P.; Daudey, J. P.; Malrieux, J. P. *J. Am. Chem. Soc.* **1981**, *103*, 4007.
(45) Astheimer, H.; Haase, W. *J. Chem. Phys.* **1986**, *85*, 1427.
(46) Handa, M.; Koga, N.; Kida, S. *Bull. Chem. Soc. Jpn.* **1988**, *61*, 3835.

Table 8. Orbital Exponents (Contraction Coefficients in Double-ζ Expansion Given in Parentheses) and Energies Used in the Extended Hückel Calculations

atom	orbital	ζ_i (c_i)	H_{ii} (eV)
O	2s	2.275	−32.30
	2p	2.275	−14.80
N	2s	1.950	−26.00
	2p	1.950	−13.40
C	2s	1.625	−21.40
	2p	1.625	−11.40
H	1s	1.300	−13.60
Ni	4s	1.825	−9.11
	4p	1.125	−5.15
	3d	5.750 (0.5683)	−13.40
		2.000 (0.6292)	

Table 9. Calculated Gaps (in meV) between the Symmetric and Antisymmetric Combinations of the d_{xy} and d_{z^2} Orbitals, Δ_{xy} and Δ_z, with Different Sets of Axial (A_i) and Equatorial (E_i) Donor Atoms at each Ni Atom (the N- and O-Donors Belong to NH_3 and H_2O Ligands, Respectively)

equatorial (*xy*)		axial (*z*)			
E_1	E_2	A_1	A_2	Δ_{xy}	Δ_z
O	O	O	O	86	36
N	O	O	O	92	47
N	N	O	O	122	34
O	O	N	O	86	68
N	O	N	O	84	68
N	N	N	O	122	47
O	O	N	N	85	64
N	O	N	N	96	70
N	N	N	N	121	62

tions[47] (atomic parameters used are given in Table 8). Even if such calculations do not explicitely include two-electron interactions, the resulting description of the molecular orbitals is expected to be qualitatively similar to that one could obtain from more sophisticated calculations. The calculated gaps are presented in Table 9. There, it can be observed that an increase in the number of nitrogen donor atoms in the coordination sphere of Ni results in an increase in the Δ values, with a larger effect on Δ_{xy} than on Δ_z. There is an increase in the value of the equatorial gap Δ_{xy} when the number of equatorial N donors is increased, and a similar behavior with respect to the axial donor set is observed for the Δ_z gap. A deviation from such idealized behavior appears when mixed donor sets are introduced in the equatorial or the axial positions, since the symmetry is lowered and the *xy* and z^2 orbitals are no longer independent. Since the results of the EH calculations are in excellent qualitative agreement with the observed trends (see Tables 6 and 7), we can now go one step further and try to understand how can the terminal ligands modulate the energy splitting of the SOMO's.

The SOMO's can be described as resulting from the interaction of the fragment orbitals (FMO's) of the bridging oxalato ligand (b_{2u}, b_{1g}, a_{1g}, and b_{3u}) with those of the fragment formed by the two metal atoms with their peripheral ligands (Scheme 2). The resulting gaps Δ_{xy} and Δ_z are due to the different interaction of the g and u combinations of the *xy* and *z* FMO's with the adequate orbitals of the bridge. Whatever can make such interactions stronger should result in a larger gap and, consequently, a stronger antiferromagnetic coupling.

The replacement of oxygen donor atoms of the terminal ligands by less electronegative nitrogen or sulphur atoms produces two main changes at the orbital level: (i) an increase of energy of the atomic orbitals of the donor atoms (represented by the ionization potentials H_{ii} within the EH framework), and (ii) a more diffuse character of their atomic orbitals (modulated by the Slater exponent ζ in the EH calculations). We have analyzed the effect of these two factors on the Δ_{xy} and Δ_z gaps separatedly by using the model compound of Scheme 1 with NH_3 ligands on all the terminal coordination sites. In a first set of calculations, the ionization energy of the nitrogen p orbitals (H_{pp}) was varied, the Slater exponent (ζ_p) being kept constant. In a second set of calculations, the Slater exponent ζ_p of the nitrogen atoms was varied with H_{pp} constant. The results are plotted in Figure 5, where the typical parameters for N and O atoms are indicated by arrows. Notice that the dependence of Δ_i on the diffuseness of the atomic orbitals may be exaggerated because Ni−N distances were kept constant in the calculations, although check calculations indicate that small changes in those distances affect little the calculated gaps. The effect of the orbital diffuseness is also found if the peripheral quantum number is increased (replacing the H_2O ligands by H_2S increases Δ_{xy} from 86 to 252 meV). Two main conclusions can be drawn from Figure 5: (i) Δ_{xy} is the leading term in all cases, and (ii) the diffuseness and ionization potential affect Δ_i in the same way, with the latter being less important. In summary, the more electronegative terminal donor atoms give smaller gaps.

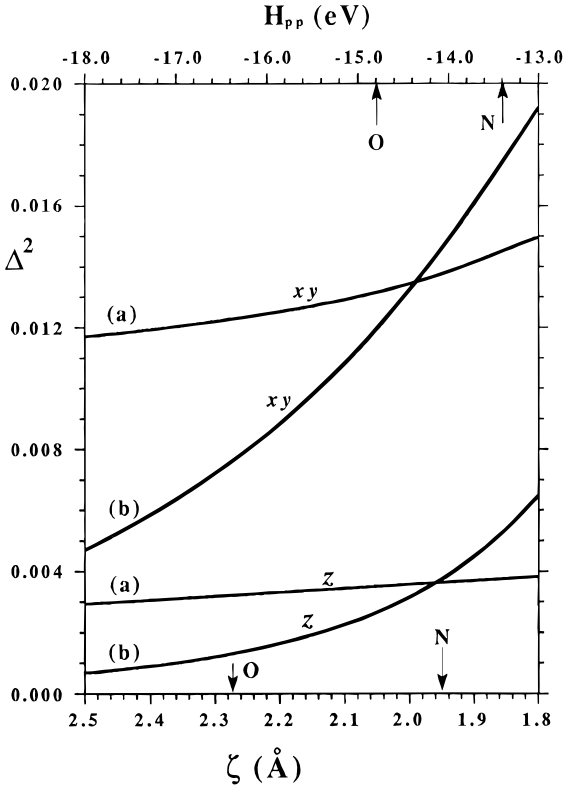

Figure 5. Plot of Δ^2 against H_{pp} and ζ when (a) H_{pp} is varied and ζ = 1.95 and (b) ζ is varied and H_{pp} = −13.4 eV. For comparative purposes, the positions of N and O atoms are indicated after their corresponding H_{pp} (−13.4 and −14.8 eV, respectively) and ζ (2.275 and 1.95, respectively) values.

The question at hand now is how these factors of the terminal ligand can affect the interaction between the metal FMO's (i.e., xy_i and z_i, Scheme 2) and the bridging ligand orbitals. According to orbital interaction rules,[48] the extent of such interactions depends on (a) the energy match and (b) the overlap between interacting orbitals. Let us look first at the energetic factor. The less electronegative terminal ligands interact in a more efficient way with the metal d orbitals because of a better energy match. Since the relevant FMO's (xy_g, xy_u, z_g, and z_u) are the metal−terminal ligand antibonding combinations, the less

(47) EH calculations were made with CACAO: Mealli, C.; Proserpio, D. M. *J. Chem. Educ.* **1990**, *67*, 399.

(48) Albright, T. A.; Burdett, J. K.; Whangbo, M.-H. In *Orbitals Interactions in Chemistry*; Wiley: New York, 1985.

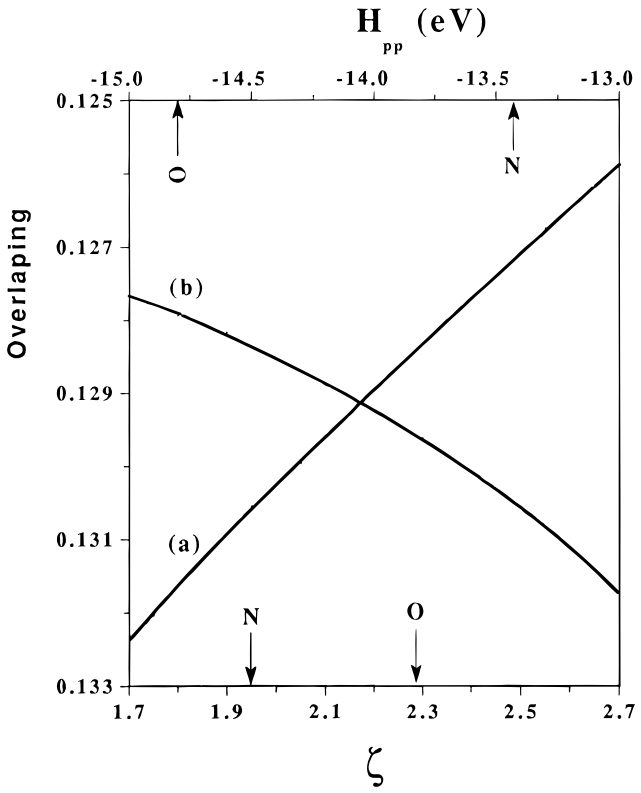

Figure 6. Plot of the overlap integral between the *xy* FMO of the $[Ni(NH_3)_4]^{2+}$ entity and the b_{2u} orbital of oxalato (a) as a function of H_{pp} ($\zeta = 1.95$) and (b) ζ ($H_{pp} = -13.4$ eV) for the N atom.

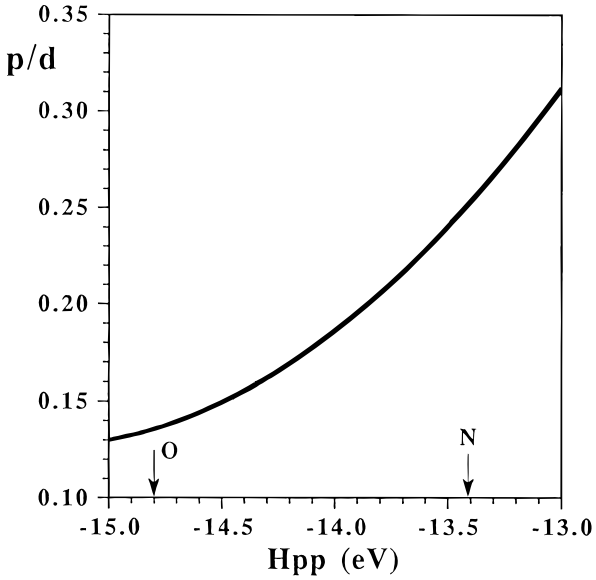

Figure 7. Plot of the p_y/d_{xy} metal orbitals ratio of the $[Ni(NH_3)_4]^{2+}$ fragment as a function of the ionization potential of the equatorial N atoms ($\zeta = 1.95$).

Scheme 3

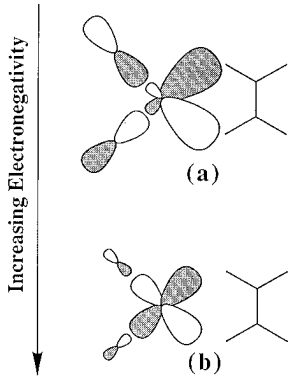

electronegative ligands should destabilize these orbitals more, making for a poorer energy match with the orbitals of the bridge and, hence smaller gaps for the SOMO's. Thus, the changes in orbital energies induced by the terminal ligands cannot account for the experimental trends and the calculated gaps. This is in contrast with the effect of atomic substitutions at the bridging ligand, which correctly explain the differences in the experimental antiferromagnetic coupling constants for different bridges (oxalato, oxamato, oxamidato, dithiooxalato, and tetrathiooxalato).[12a]

It becomes clear that the different gaps obtained for different donor sets as the terminal positions must be related to different overlap between the metal and the bridging ligand orbitals. This effect is clearly illustrated by plotting the overlap integral between the *xy* FMO of the NiL_4 group and the b_{2u} orbital of the oxalato bridge as a function of the electronegativity and of the diffuseness of the p atomic orbital of the terminal ligands (Figure 6). Since this is a counterintuitive effect, a detailed analysis of the overlap between the FMO's is in order. Let us look first at the interaction between the xy_i FMO's and the b_{1g} and b_{2u} orbitals of the bridging ligand. It can be shown that the major effect of the changes in the orbital energy and the diffuseness of the N-2*p* orbitals on xy_g and xy_u is a varying degree of hybridization of the latter. It is generally true that the FMO's with a major contribution from the metal d orbitals are metal−ligand antibonding, and lose part of their antibonding character through hybridization away from the ligands. The metal−ligand interaction is stronger, and the hybridization is consequently larger for less electronegative ligands (Scheme 3). This effect can be appreciated in Figure 7, where the relative weight of the p_y and d_{xy} metal orbitals in the corresponding FMO of the $[Ni(NH_3)_4]^{2+}$ fragment is plotted as a function of the ionization potential of the equatorial N atoms. More diffuse atomic orbitals at the equatorial donors also enhance hybridization. Hence, the less electronegative equatorial ligands, which interact more strongly with the nickel d orbitals, induce a strong hybridization toward the bridging ligand, thus favoring larger *xy*/bridge orbital overlap. These ideas are in keeping with previous theoretical studies in which the singlet−triplet separations were calculated for compounds $[Cu_2(\mu\text{-}OMe)_2X_2(NH_3)_2]$, and found to increase from $X = F^-$ (-786 cm^{-1}) to $X = Br^-$ (-1358 cm^{-1}), although no explanation was given for such a trend.[45] Given the nodal characteristics of the d_{xy} orbital, the axial ligands cannot induce hybridization of this orbital; hence, the Δ_{xy} gap is not affected by the nature of the axial ligands (Table 9).

In a similar way, stronger axial donors induce hybridization of the d_{z^2} orbital in the *xy* plane, thus favoring interaction with the orbitals of the bridging group and larger Δ_z gaps. The equatorial ligands, on the other hand, also rehybridize the z^2 orbital, both outwards in the *xy* plane (through p + d mixing) and along the *z* direction (through s + d mixing), resulting in practically the same overlap with the FMO's of the bridging ligand regardless of the nature of the peripheral ligands.

From the present investigation we can conclude that, although the unpaired electrons are essentially localized on the 3d orbitals of the metal ions, some spin density occurs on the 4p orbitals. Such 4p spin density is associated with d-orbital hybridization and a stronger metal−bridging ligand overlap. Hence, the 4p spin density must be correlated to the strength of the antiferromagnetic coupling interaction. In this regard, it is interesting to mention the work carried out by Figgis *et al.*[49] on the theoretical and experimental (polarized neutron diffraction experiments) determination of spin densities in mononuclear

complexes of transition metal ions. They observed a significant amount of spin density on the 4p metal orbitals. More recently, Verdaguer *et al.*[50] have studied the magnetic dichroic properties of the compounds $Cs^{I}A^{II}[Cr^{III}(CN)_6]$ with A = Ni or Mn. These authors recorded X-ray magnetic circular dichroism at the K and L edges of the transition metal ions in the magnetically ordered phase and detected an intense dichroic signal in the energy range corresponding to the allowed transition to p-symmetry levels of the metal (4p orbitals), due to a spin polarization of the 4p orbitals of the absorbing metal ions by the surroundings. In summary, the present work, together with the experimental data from other authors, demonstrates that the magnetic interactions between transition metal ions can be properly explained by considering not only the *n*d orbitals of the metal atoms, but also the participation of their $(n + 1)$s and $(n + 1)$p orbitals.

Acknowledgment. This work was in part supported by the UPV/EHU (Grant No. 169.310-EA004/93), the DGICYT (Grant PB92-0655 and Project PB91-0807-C02-01) and the Human Capital and Mobility Program from the EEC (Network on Magnetic Molecular Materials trhough Contract ERBCH-RXDCT920080). C.G.-M. and J.C. acknowledge financial support from the Departamento de Educación del Gobierno Vasco and Conselleria d'Educació i Ciència de la Generalitat Valenciana, respectively, for predoctoral grants.

Supporting Information Available: Tables of crystallographic data, thermal parameters for non-hydrogen atoms, hydrogen coordinates, and a listing of bond lengths, bond angles, hydrogen contacts, least-squares planes, and dihedral angles for **1** and **2** (14 pages). Ordering information is given on any current masthead page.

IC951081G

(49) (a) Figgis, N. B.; Reynolds, P. A.; White, A. H. *J. Chem. Soc., Dalton Trans.* **1987**, 1737. (b) Graham, S. C.; Deeth, R. J.; Figgis, B. N.; Philips, R. A. *Inorg. Chem.* **1987**, *26*, 101. (c) Christos, G. A.; Figgis, B. N.; Philips, A. R. *J. Chem. Soc., Dalton Trans.* **1990**, 2947.

(50) Verdaguer, M.; Mallah, T.; Helary, C.; L'Hermite, F.; Sainctavit, P.; Arrio, M. A.; Babel, D., Baudelet, F.; Dartyge, E.; Fontaine, A. *Physica* **1995**, *B209*, 765−767.